Synthesis, crystal structure, and magnetic properties of the manganate $La_2Ca_2MnO_6(O_2)$ related to the hexagonal perovskite-type structure

E. Gaudin, G. Goglio, A. Besnard, and J. Darriet[*]

Institut de Chimie de la Matière Condensée de Bordeaux (ICMCB), UPR9048 CNRS, Université Bordeaux 1, 87 Avenue du Docteur Schweitzer, Pessac Cedex 33608, France

Abstract

The compound $La_2Ca_2MnO_6(O_2)$ has been synthesized from $La_2Ca_2MnO_7$ heated at 1123 K under high pressure (4 GPa) with $KClO_3$ as oxygen source. The crystal structure has been refined from X-ray powder data in the $R\bar{3}m$ space group. The unit-cell parameters are $a = 5.6335(2)$ Å and $c = 17.4879(8)$ Å. Perpendicular to the c-axis, the structure is built up by the periodic stacking of two close packed $[LaO_3]$ layers separated by a layer of composition $[Ca_2O_2]$ containing $(O_2)^{2-}$ peroxide ions. This oxide belongs to the family of compounds formulated as $[A'_2O_{2-\delta}][A_nB_{n-1}O_{3n}]$ for $n = 2$ and $\delta = 0$. It is the first member of the series where the thickness of the perovskite slab corresponds to one $[BO_6]$ ($B = Mn$) octahedron. The structural relationships with $La_2Ca_2MnO_7$ are discussed and the magnetic properties show that in both phases manganese is tetravalent.
© 2003 Elsevier Science (USA). All rights reserved.

Keywords: Oxygen pressure; Hexagonal perovskite; Stoichiometry; Rietveld refinement; Magnetic properties

1. Introduction

A reinvestigation of the Ba–Ru–O system has revealed in addition to the well-known $BaRuO_3$ hexagonal perovskite, the existence of the phases $Ba_4Ru_3O_{10}$, $Ba_5Ru_3O_{12}$, $Ba_5Ru_2O_{10}$ and $Ba_5Ru_2O_9(O_2)$ [1–4]. These two latter compounds derive from the hexagonal perovskite-type structure by the stacking of mixed $[BaO_3]$ and $[Ba_2O_{2-\delta}]$ layers. $Ba_5Ru_2O_{10}$ and $Ba_5Ru_2O_9(O_2)$ correspond to $\delta = 1$ and 0, respectively. For $\delta = 0$, the two oxygen atoms are grouped in pair like in peroxide ions. As it has been shown by magnetic measurements, the main characteristic of these two phases is that the valence state of ruthenium is pentavalent whatever the δ value may be [4]. $Ba_5Ru_2O_{10}$ and $Ba_5Ru_2O_9(O_2)$ correspond to the $n = 3$ member of the general series $[A'_2X_{2-\delta}][A_nB_{n-1}X_{3n}]$ (A, $A' = Ba$, $B = Ru$ and $X = O$) in which n represents the number of consecutive $[AX_3]$ layers in the perovskite slabs [3,4]. TG experiments have shown that $Ba_5Ru_2O_9(O_2)$ is not stable thermally and loses one oxygen giving rise to the compound $Ba_5Ru_2O_{10}$. Recently, the new manganate $La_2Ca_2MnO_7$ has been discovered which corresponds to the $n = 2$ and $\delta = 1$ member of the series [5]. In this case the thickness of the perovskite slabs is only one octahedron separated by a layer of composition $[Ca_2O]$. In line with the results observed for the ruthenates, we wonder how we can expect to isolate the new "oxidized" phase $La_2Ca_2MnO_6(O_2)$ corresponding to $n = 2$ and $\delta = 0$. This is possible if the preparations are carried out in oxidizing atmosphere and under high pressure. This paper is devoted to the preparation, crystal structure and magnetic properties of this new oxide. We will emphasize that the basic principles proposed for the ruthenate series can be applied to these manganates.

2. Experimental

2.1. Samples preparation

2.1.1. $La_2Ca_2MnO_7$

A mixture of decarbonated La_2O_3, $CaCO_3$, manganese acetate and citric acid with the molar ratio 1.05:2.1:1:1.2 has been dissolved in nitric acid

---

[*]Corresponding author. Fax: +33-5-56-84-2761.
E-mail address: darriet@icmcb.u-bordeaux.fr (J. Darriet).

Table 1
Structural parameters for $La_2Ca_2MnO_7$

Position		Wang et al.					This paper					
Space group		$R\bar{3}$					$R\bar{3}m$					
Cell param.		$a = 5.62176(4)$ Å					$a = 5.61715(13)$ Å					
		$c = 17.3161(2)$ Å					$c = 17.3521(4)$ Å					
Position	Site	x	y	z	Frac.	Site	x	y	z	B_{iso} (Å^2)	Frac.
Mn1	$1a$	0	0	0	1	$3a$	0	0	0	0.11(5)	1
La1	$6c$	0	0	0.37757(3)	0.933	$6c$	0	0	0.37753(4)	0.12(2)	0.939(2)
Ca1	$6c$	0	0	0.37757	0.077	$6c$	0	0	0.37753	0.12	0.061
Ca2	$6c$	0	0	0.82745(7)	0.933	$6c$	0	0	0.82735(11)	0.68(5)	0.939
La2	$6c$	0	0	0.82745	0.077	$6c$	0	0	0.82735	0.68	0.061
O1	$18f$	0.0148(4)	0.502(3)	0.6024(1)	1	$18h$	0.0138(10)	0.5069	0.6018(2)	1.18(8)	1
O2	$18f$	0[a]	0.128(1)	0.5[a]	1/3[a]	$18g$	0	0.129(2)	1/2	1[a]	1/6[a]

[a] Fixed in the refinement.

Table 2
Refinement results for various occupancies and B_{iso} values for O2 position for $La_2Ca_2MnO_7$

Formula	Occupancy	B (Å^2)	R_I (%)	R_p (%)	R_{wp} (%)
$La_2Ca_2MnO_7$	1/6[a]	−1.9(4)	2.24	6.92	9.68
$La_2Ca_2MnO_8$	1/3[a]	31(2)	3.03	7.28	10.16
$La_2Ca_2MnO_{7.09}$	0.182(4)	1[a]	2.28	6.94	9.70
$La_2Ca_2MnO_{7.02}$	0.170(4)	−1.7(4)	2.24	6.92	9.67
$La_2Ca_2MnO_7$	1/6[a]	1[a]	2.32	6.95	9.71

[a] Fixed.

($c \sim 1.6$ mol L^{-1}). After evaporation of water the mixture has been pre-heated at 600°C in a furnace under an oxygen flow to facilitate the evaporation of the nitrous vapors. The fine powder obtained was heated at 1173 K for 12 h. The powder was then grounded and heated in an alumina crucible twice 12 h at 1423 K with intermediate regrinding. Starting from a stoichiometric ratio of La_2O_3, $CaCO_3$ and manganese acetate, the impurity $(La, Ca)MnO_3$ has been observed in the X-ray pattern. The amount of this impurity has significantly reduced by the use of a small excess of La_2O_3 and $CaCO_3$ (5% molar) in the starting mixture.

2.1.2. $La_2Ca_2MnO_8$

$La_2Ca_2MnO_8$ has been prepared from $La_2Ca_2MnO_7$ heated under high oxygen pressure in a belt-type apparatus with a bore diameter of 12 mm according to the following reaction:

$$La_2Ca_2MnO_7 + KClO_3$$
$$\xrightarrow{P,T} La_2Ca_2MnO_8 + KCl + O_2\uparrow.$$
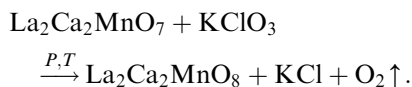
$La_2Ca_2MnO_7$ and the oxygen source $KClO_3$ were ground with a 1:1 molar ratio in an agate mortar. The obtained powder was packed into a platinum capsule insulated from the graphite microfurnace with pyrophyllite. This assembly was then loaded into the high-

pressure chamber. Sample was first subjected to pressure of 4 GPa, heated to temperature of 1123 K during 4 min then cooled down to room temperature and finally decompressed.

Moreover, in order to confirm that all the evolutions observed on the XRD pattern and TG analysis can be attributed to the insertion of oxygen in the structure nor to structural modifications induced by pressure, a sample of $La_2Ca_2MnO_7$ was submitted to the same pressure and temperature treatment without adding oxygen source (4 GPa, 1123 K during 4 min).

2.2. Thermogravimetric analysis

Thermogravimetric analysis were performed on a MTB10-8 SETARAM balance with an accuracy of $\Delta m = 0.01$ mg. Experiments were carried out under an Ar–5%H$_2$ atmosphere from room temperature up to 950°C. The starting masses of $La_2Ca_2MnO_7$ and $La_2Ca_2MnO_8$ were 252 and 89 mg, respectively.

2.3. X-ray diffraction

X-ray powder diffraction data of all the products were collected at room temperature over the angular range $5° \leqslant 2\theta \leqslant 120°$ with a step size of $\Delta(2\theta) = (0.02)°$ using a Philips X-pert.

All the X-ray diffraction data were refined by a profile analysis using the Jana2000 program package [6]. The background was estimated by a Chebyshev polynomial and the peak shapes were described by a standard pseudo-Voigt function. The refinement of peaks asymmetry was performed using four parameters.

2.4. Magnetic measurements

Magnetic measurements were performed using a Quantum Design SQUID magnetometer. The susceptibility for both compounds was recorded in a field of 1 T
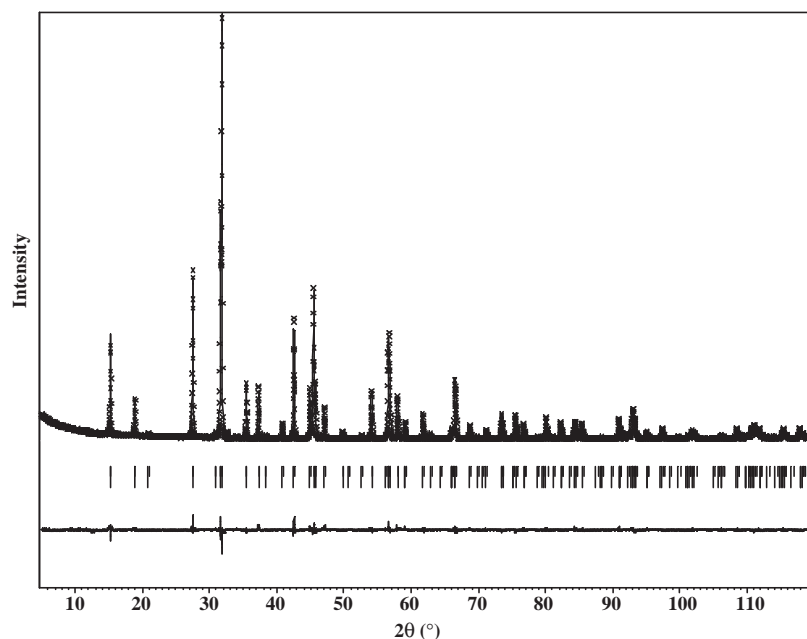
Fig. 1. Final profile refinement for $La_2Ca_2MnO_7$: observed (cross), calculated (full line), and difference (bottom) profiles. Reflection positions are indicated by tick marks.

where the magnetization is linear with the field in the whole temperature range (2–350 K).

3. Results

3.1. Thermogravimetric analysis and structural characterization

3.1.1. $La_2Ca_2MnO_7$

The aim of the Rietveld refinement on our powder sample was to confirm the oxygen stoichiometry proposed by Wang et al. [5]. The Rietveld refinement was performed with the JANA2000 program [6]. In a first step a Le Bail refinement was done to establish the lattice parameters, peak profiles (classical pseudo-Voigt function) and background (Chebyschev function). This full pattern-matching refinement led to the global residual profile value $R_p = 0.064$ and weighted profile value $R_{wp} = 0.092$. The atomic positions proposed by Wang et al. in the space group R-3 were used as starting model. The positions they found for both oxygen sites suggest a higher symmetry for the structure. Here, by using the more symmetrical $R\bar{3}m$ space group the structure (Table 1) was refined with less correlations. A small disorder between La and Ca atoms at the La1 and Ca1 positions has been observed as ever reported by Wang et al. [5]. The substitution ratio is equal to 6.1%. As previously pointed by Grasset et al. [3,4] the occupancy of the oxygen position (O2 position) corresponding of the $[Ca_2O_{2-\delta}]$ layer should be carefully analyzed. If the occupancy of O2 position is equal to 1/6
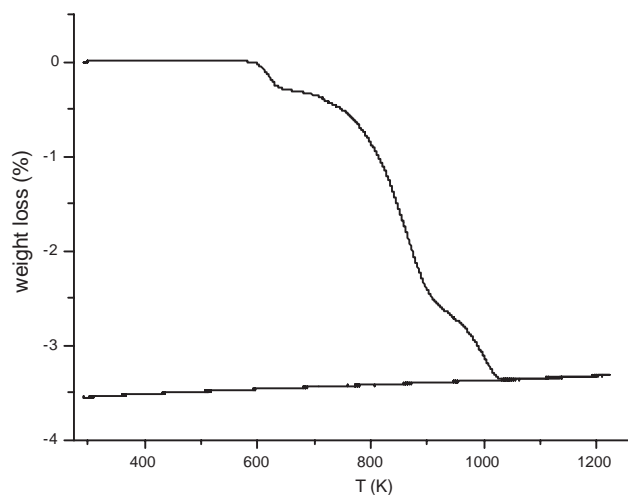

Fig. 2. TGA under $Ar–5\%H_2$ atmosphere of $La_2Ca_2MnO_7$.

or 1/3 then the layer has the composition $[Ca_2O]$ or $[Ca_2O_2]$ and the sample has the formula $La_2Ca_2MnO_7$ or $La_2Ca_2MnO_8$, respectively. In Table 2, the different combinations tested for the occupancy and the displacement parameter are summarized. It is clear from these results that the O2 occupancy is very close to 1/6. Indeed, the value refined for B_{iso} with the O2 occupancy fixed to 1/3 is huge (see Table 2). Because of the strong correlations between the occupancy and the displacement parameter of O2 position for the final refinement the B_{iso} parameter has been fixed to 1 and the occupancy to 1/6 (Table 2 and Fig. 1).

The thermogravimetric experiment under $Ar–5\%H_2$ shows a mass loss of 3.55% (Fig. 2). From the

analysis of the X-ray diffractogram of the product after reduction the following reaction has been deduced:

$$La_2Ca_2MnO_7 \rightarrow La_2O_3 + 3Ca_{2/3}Mn_{1/3}O + H_2O.$$
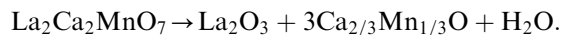
$Ca_{2/3}Mn_{1/3}O$ corresponds to a solid solution between CaO and MnO. The cell parameter of this cubic phase $a = 4.6960$ Å is consistent with a ratio of 66% of CaO and 33% of MnO from the Vegard law found in the Arean and Stone work [7] on the CaO–MnO solid solution. The theoretical loss from this reduction reaction would be 3.05%, which is close to the experimental value of 3.55% (Fig. 2). A small excess of oxygen in the as-prepared compound can explain the difference observed between the two values. Within the

Table 3
Structural parameters for $La_2Ca_2MnO_8$

Space group	$R\bar{3}m$					
Cell param.	$a = 5.6335(2)$ Å, $c = 17.4879(8)$ Å					
Position	Site	x	y	z	B_{iso} (Å^2)	Frac.
Mn1	3a	0	0	0	0.31(6)	1
La1	6c	0	0	0.37492(5)	0.38(2)	0.899(2)
Ca1	6c	0	0	0.37492	0.38	0.101
Ca2	6c	0	0	0.82724	0.40(6)	0.899
La2	6c	0	0	0.82724(13)	0.40	0.101
O1	18h	0.0177(10)	0.5089(5)	0.6035(2)	0.57(9)	1
O2	18g	0	0.1441(15)	1/2	0.2(3)	1/3

experimental errors this result has also been observed in the Rietveld refinement (Table 2).

3.1.2. $La_2Ca_2MnO_8$

The Rietveld refinement was carried out using the previous structural results as starting model. As expected a significant change has been observed only for the O2 position occupancy. For an occupancy of 1/3 of O2 position the refinement gave the profile fit factors $R_p/R_{wp} = 0.077/0.116$ and residual factors $R/R_w = 0.030/0.034$ with B_{iso} value of O2 position equal to 0.2 Å^2 (Table 3 and Fig. 3). If the occupancy of O2 position is fixed to 1/6 the B_{iso} value is negative ($B_{iso} = -4.5(3)$ Å^2) with $R_p/R_{wp} = 0.081/0.118$ and $R/R_w = 0.034/0.038$. The refinement indicates clearly that the occupancy is close to 1/3 confirming the stoichiometry of the phase. As for $La_2Ca_2MnO_7$ a small disorder has been observed between Ca and La in the two independent positions.

The mass loss observed in the thermogravimetric experiment (Fig. 4) equal to 5.85% is nearly equal to the theoretical value of 5.92% expected from the following reaction:

$$La_2Ca_2MnO_8 \rightarrow La_2O_3 + 3Ca_{2/3}Mn_{1/3}O + 2H_2O.$$
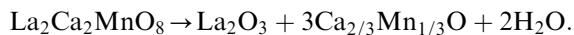
The analysis of the X-ray data shows clearly a significant increasing of the c parameter when going from $La_2Ca_2MnO_7$ to $La_2Ca_2MnO_8$, with c equal to 17.3521(4) and 17.4879(8) Å, respectively. This evolu-

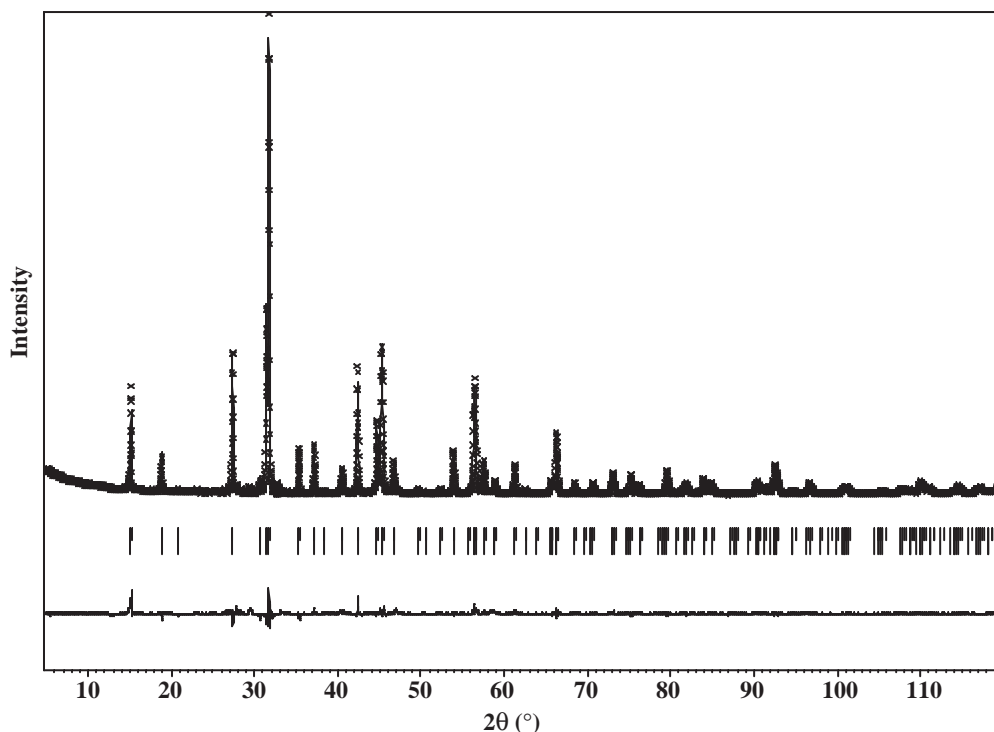

Fig. 3. Final profile refinement for $La_2Ca_2MnO_8$: observed (cross), calculated (full line), and difference (bottom) profiles. Reflection positions are indicated by tick marks.
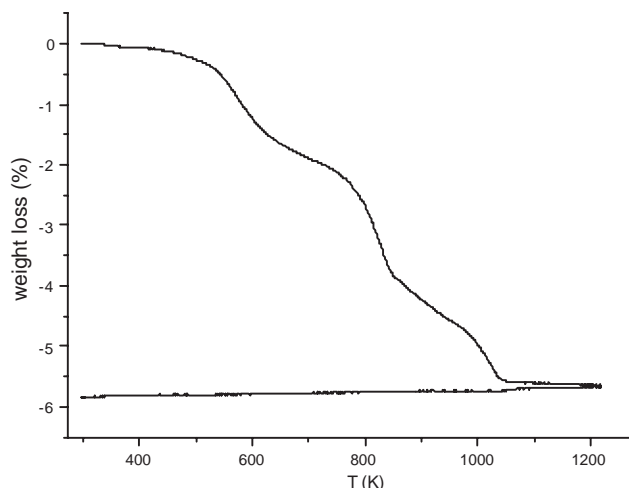
Fig. 4. TGA under Ar–5%H$_2$ atmosphere of La$_2$Ca$_2$MnO$_8$.

tion is emphasized in Fig. 5 where a part of the diffraction pattern of both compounds is displayed. Moreover, the same part of the diffraction pattern of La$_2$Ca$_2$MnO$_7$ that was submitted to pressure without oxygen source is presented. The cell parameters deduced for this sample are $a = 5.6176(2)$ and $c = 17.3175(9)$ Å. The broadening of the peaks observed can be ascribed to an amorphization of the compound and the slight reduction of the cell parameter is consistent with applying a pressure. This last experiment is an additional proof of the oxygen insertion in La$_2$Ca$_2$MnO$_7$ induced by the decomposition of KClO$_3$ under pressure.

3.2. Magnetic measurements

3.2.1. La$_2$Ca$_2$MnO$_7$

Above 100 K the magnetic susceptibility follows a Curie–Weiss law with the fitted Curie constant $C = 1.79$ emu K mol^{-1} and θ_p nearly equal to 0 (Fig. 6a). At lower temperature a sharp increase of the susceptibility up to a maximum at 3 K suggests a long-range antiferromagnetic ordering and one can consider that this temperature corresponds to the Néel temperature.

3.2.2. La$_2$Ca$_2$MnO$_8$

The same kind of evolution of the susceptibility has been observed for La$_2$Ca$_2$MnO$_8$ (Fig. 6b). However, a weak temperature-independent paramagnetism (TIP) has been introduced in the Curie–Weiss law for the fitting of the susceptibility above 150 K. The results given by this fit are $C = 1.92$ emu K mol^{-1}, $\theta_p = -2$ K and $TIP = 220.10^{-6}$ emu mol^{-1}. The maximum of the susceptibility observed at 2.5 K can be attributed to the three-dimensional antiferromagnetic ordering.
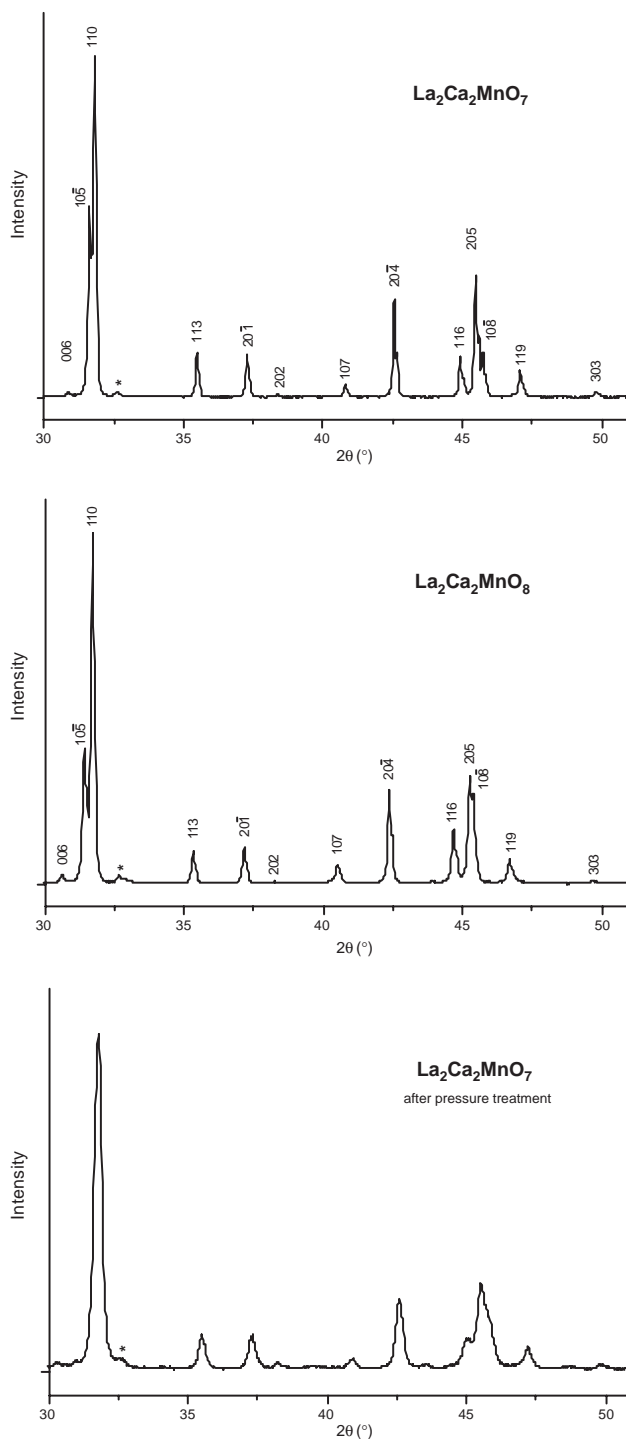

Fig. 5. X-ray diffraction profiles of La$_2$Ca$_2$MnO$_7$, La$_2$Ca$_2$MnO$_8$ and La$_2$Ca$_2$MnO$_7$ after pressure treatment from 30° to 51° (* impurity of (La, Ca)MnO$_3$).

4. Discussion

La$_2$Ca$_2$MnO$_8$ is a new member of the family with general formula $[A'_2O_{2-\delta}][A_nB_{n-1}O_{3n}]$ where $A = $ La, $A' = $ Ca, $B = $ Mn, $n = 2$ and $\delta = 1$. Its structure can be described as resulting from the stacking of two [LaO$_3$]
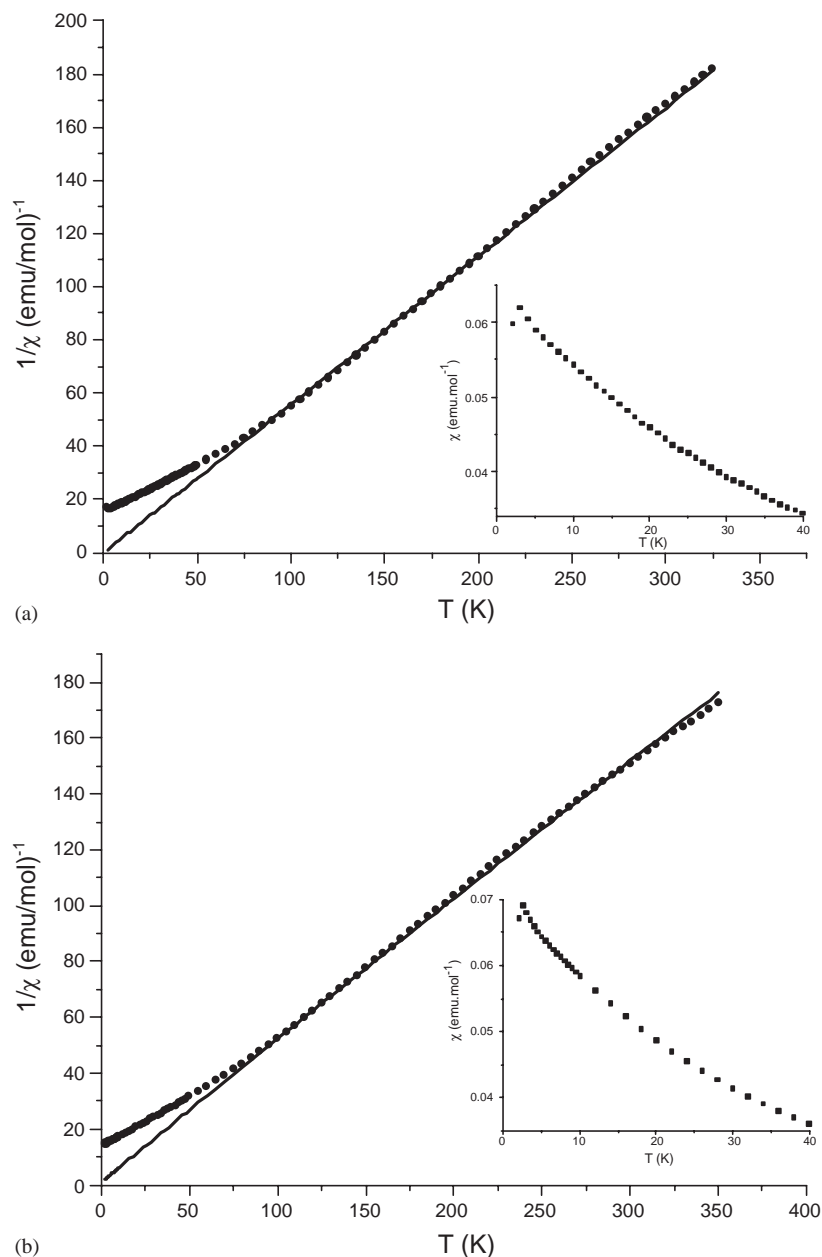
Fig. 6. Temperature dependence of the inverse molar magnetic susceptibility of (a) La$_2$Ca$_2$MnO$_7$ and (b) La$_2$Ca$_2$MnO$_8$. The fitted Curie–Weiss law for the high-temperature range is displayed. A zoomed-in view of the susceptibility curves in the low-temperature region is given in the insets.

layers and one [Ca$_2$O$_2$] layer three times along the c-axis (Fig. 7). The packing sequence of [LaO$_3$] layers along the c-axis is -a-b-Ca$_2$O$_2$-b-c-Ca$_2$O$_2$-c-a-Ca$_2$O$_2$-a-b. Manganese atoms fill the octahedral interstitial holes between two successive [LaO$_3$] layers; therefore, the calcium atoms fill trigonal prismatic interstitial sites between the [LaO$_3$] layers. The calcium environment is completed by three oxygen atoms belonging to the [Ca$_2$O$_2$] layers (Figs. 8a and 9). In the [Ca$_2$O$_2$] layers, the six oxygen atoms are grouped in pairs with a bond distance of 1.624(12) Å (Table 4), this distance is close to the one observed for Ba$_5$Ru$_2$O$_9$(O$_2$), 1.554 Å [3]. These

oxygen pair distances are characteristic of peroxide ions (O$_2$)$^{2-}$ and are comparable to the O–O distance found in Ba$_2$O$_2$, 1.49 Å [8]. Then the main structural difference induced by the oxygen insertion in La$_2$Ca$_2$MnO$_7$ is the replacement of the [Ca$_2$O] layer by the [Ca$_2$O$_2$] layer leading to the new compound La$_2$Ca$_2$MnO$_8$. From a structural point of view this stoichiometric change is observed through the occupancy factor of the O2 position in the [Ca$_2$O$_2$] layer (Fig. 9). The lanthanum atom is surrounded by nine oxygen atoms with La–O distances equal to 2.508(5) and 2.843(4) Å and by one peroxide ion with La–O distance equal to 2.333(3) Å
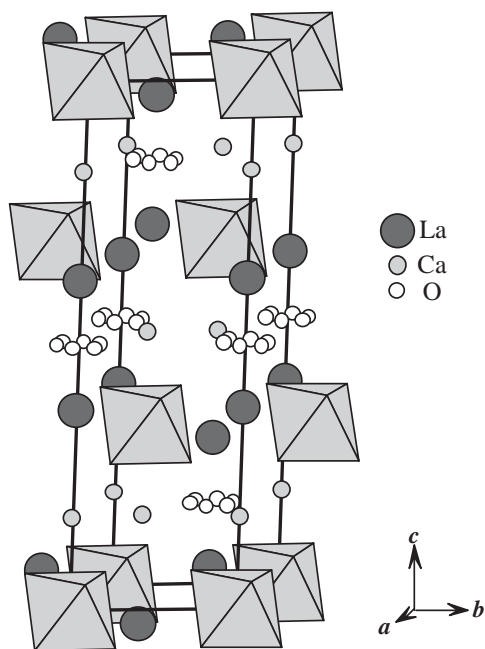
Fig. 7. View of the structure of $La_2Ca_2MnO_8$. The [MnO_6] octahedra are outlined.

(Fig. 8b and Table 4). For the MnO_6 octahedra, the Mn–O distance, 1.895(6) Å, is close to the values previously observed in $SrMnO_3$, 1.872 and 1.906 Å [9] and reported by Shannon, 1.93 Å [10].

The replacement of one oxygen O^{2-} by a peroxide ion $(O_2)^{2-}$ in $La_2Ca_2MnO_7$ would not change the oxidation degree of manganese in $La_2Ca_2MnO_8$ and the following charge balance can be expected: $La_2^{+III}Ca_2^{+II}Mn^{+IV}$ $O_6^{-II}(O_2)^{-II}$. The bond valence calculation using Brown and Altermatt values [11] gives a BV sum of 4.09 for manganese, close to the value expected. This assumption is also confirmed by the magnetic measurements. Indeed, the Curie constants found for $La_2Ca_2MnO_7$ and $La_2Ca_2MnO_8$, 1.79 and 1.92 emu K mol^{-1}, respectively, are very close to the theoretical expected spin-only Curie constant $C = 1.875$ emu K mol^{-1} calculated for Mn^{4+} ($S = 3/2$). The synthesis of $La_2Ca_2MnO_8$ from $La_2Ca_2MnO_7$ under high oxygen pressure induces an insertion of oxygen and cannot be considered as an oxidation reaction.

At this time only few members of this new family of compounds with the general formula $[A'_2O_{2-\delta}]$ $[A_nB_{n-1}O_{3n}]$ have been identified. One can notice the existence of some compounds of this family in the Ba–Nb–S and Ba–Ta–S systems, with $n = 3$ and 4 (see [4] for instance and references therein).

The [Ca_2O] layer can be related to the [NaO] layer observed in β alumina (Na_2O, $11Al_2O_3$). It is well known that perpendicular to the c hexagonal axis the structure of the β alumina can be described by the stacking of spinel slabs separated by a layer of composition [NaO] [12–15]. In fact, this last one results from a layer of composition
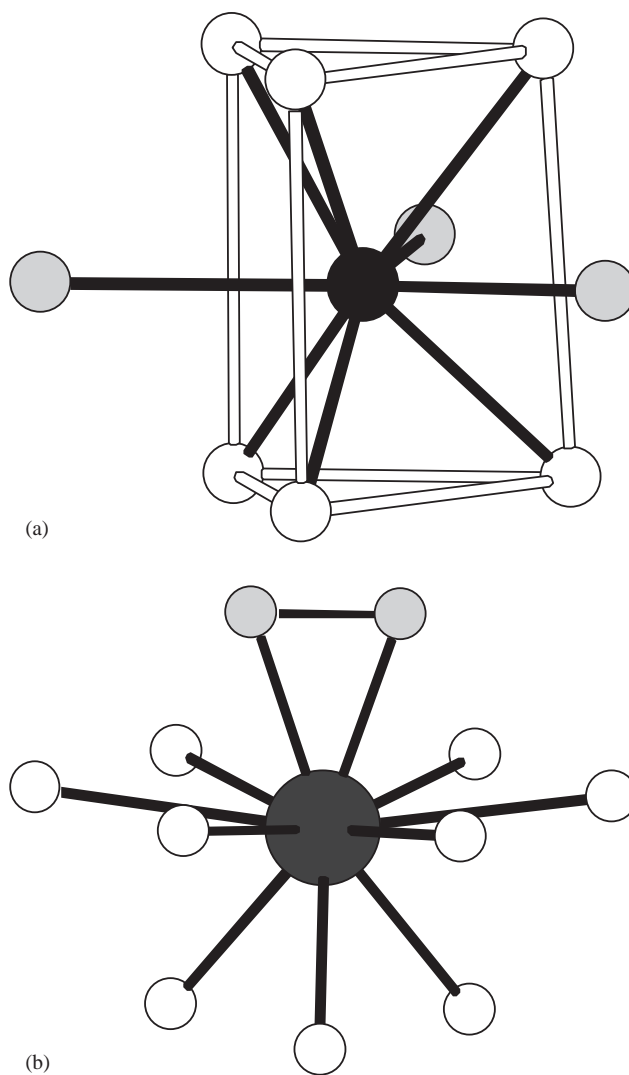

Fig. 8. Environment of (a) the calcium atoms and (b) the lanthanum atoms in $La_2Ca_2MnO_8$. The O1 position is represented by open circle and the O2 position by filled circle.
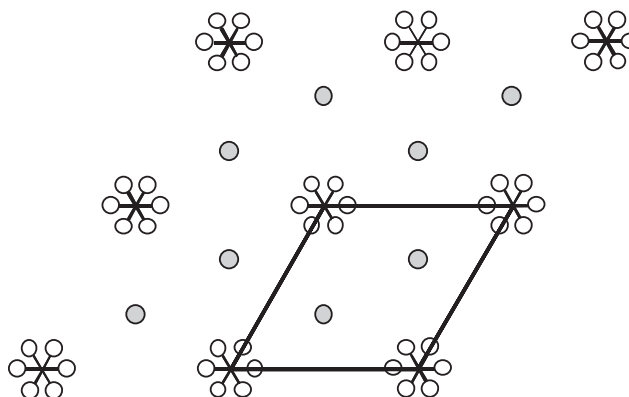

Fig. 9. View of the [Ca_2O_2] layer perpendicular to the c-axis.

[Na_2O] where only 50% of the sodium position is occupied giving rise to the well-known high ionic conductivity of β alumina. Considering the full occupancy of the sodium

Table 4
Main interatomic distances (Å) and s.u. in $La_2Ca_2MnO_8$

La1	O1 × 3	2.508(5)	Mn1	O1 × 6	1.895(6)
	O1 × 6	2.843(4)			
	O2 × 2	2.333(3)	O2	O2 × 2	1.406(11)
				O2 × 2	1.624(12)
Ca2	O1 × 3	2.415(5)			
	O1 × 3	2.458(5)			
	O2 × 3	2.584(7)[a]			

[a] Shortest distance Ca–O2.

position, it appears that the $[Na_2O]$ and $[Ca_2O]$ layers are similar. Both structure are hexagonal with similar a parameter ($a \approx 5.8$ Å) and built up of mixed layers perpendicular to the *c*-axis: for β alumina the mixed layers have composition $[O_4]$ (spinel blocks) and $[A'_{2-\delta'}O]$ with $A' = Na$ and $\delta' = 1$ and in $La_2Ca_2MnO_7$, the composition of the two types of mixed layers is $[AO_3]$ ($A = Ca/La$) and $[A'_{2-\delta'}O]$ with $A' = Ca/La$ and $\delta' = 0$, respectively. To conclude, the structural relationships between these two phases open a new route for the synthesis of new compounds with particular properties as generator of oxygen source with simultaneously ionic conductivity.

References

[1] C. Dussarrat, F. Fompeyrine, J. Darriet, Eur. J. Solid State Inorg. Chem. 31 (1994) 289.
[2] C. Dussarrat, F. Grasset, R. Bontchev, J. Darriet, J. Alloys Compds. 233 (1996) 15.
[3] F. Grasset, C. Dussarrat, J. Darriet, J. Mater. Chem. 7 (9) (1997) 1911.
[4] F. Grasset, M. Zakhour, J. Darriet, J. Alloys Compds. 287 (1999) 25.
[5] Y. Wang, J. Lin, Y. Du, R. Qin, B. Han, C.K. Loong, Angew. Chem. Int. Ed. 39 (15) (2000) 2730.
[6] V. Petricek, M. Dusek, JANA2000. Institute of Physics, Czech Academy of Sciences, Prague, Czech Republic, 2000.
[7] C.O. Arean, F.S. Stone, J. Chem. Soc. Faraday Trans—I 75 (1979) 2285.
[8] W. Wong-Ng, R.S. Roth, Physica C 233 (1994) 97.
[9] P.D. Battle, T.C. Gibb, C.W. Jones, J. Solid State Chem. 74 (1988) 60.
[10] R.D. Shannon, Acta Crystallogr. A 32 (1976) 751.
[11] I.D. Brown, D. Altermatt, Acta Crystallogr. B 41 (1985) 244.
[12] W.L. Bragg, C. Gattfried, J. West, Z. Kristallogr. 77 (1931) 255.
[13] C.A. Beevers, M.A.S. Ross, Z. Kristallogr. 97 (1937) 59.
[14] J. Felsche, Naturwissenschaften 54 (1967) 612.
[15] C.R. Peters, M. Bettman, J.W. Moore, M.D. Glick, Acta Crystallogr. B 27 (1971) 1826.